

Supporting Information

Thermosensitive luminescence halloysite-based nanocomposite enabling encryptable thermal printing

Pengying Jia^{a,c}, Yelong Lu^{*a}, Yuqing Yang^a, Xiaoyan Zhu^a, Hailei Zhang^{*b}, Yonggang Wu^{*a}

^aCollege of Chemistry and Materials Science, Hebei University, Baoding, 071002, P. R. China;

^bKey Laboratory of Medicinal Chemistry and Molecular Diagnosis of Ministry of Education, Hebei University, Baoding, 071002, P. R. China.

^cCollege of Physics Science and Technology, Hebei University, Baoding 071002, China.

Correspondence

No. 180 Wusi Road, College of Chemistry and Materials Science, Hebei University, Baoding 071002, P. R. China

E-mail: wuyonggang@hbu.edu.cn (W. Y.); 15613663132@163.com (Y. L.).

No. 2666 Qiyi Road, Key Laboratory of Medicinal Chemistry and Molecular Diagnosis of Ministry of Education, Hebei University, Baoding 071000, P. R. China

E-mail: zhanghailei@hbu.edu.cn (H. Z.)

Experimental

Materials

HNTs were obtained from GuangZhouShinshi Metallurgy and Chemical Company Ltd (Guangzhou, China) and purified according to our previous work¹. The amino-modified HNTs (HNTs-NH₂) and HNTs-based photo-initiator (HNTs-I) were also prepared by referring to our previously reported². Organic solvents including ethanol, acetone, and tetrahydrofuran were purchased from Tianjin Kemiou Chemical Reagent Co., Ltd. Distilled water was used throughout the study. High-purity argon was used for degassing procedures. Printing molds were order from Alibaba Co., Ltd.

Characterizations

The morphological characterizations were performed by using a Tecnai G2 F20 S-TWIN transmission electron microscope (TEM) with an accelerating voltage of 200 kV. A JEOL Ltd. Elemental mapping images and high-resolution transmission electron microscopy (HRTEM) images of HNTs-CDs were recorded by using a JEOL JEM-ARM200F model spherical aberration transmission electron microscope.

FTIR spectra were recorded in the region of 400-4000 cm⁻¹ for each sample on a Thermo Fisher Scientific NICOTET IS10 FTIR spectrophotometer. Samples were previously ground and mixed thoroughly with KBr.

X-ray photoelectron spectroscopy (XPS) was carried out on a Thermo Scientific ESCALab 250Xi using 200 W monochromated Al K α radiation. The 500 μ m X-ray spot was used for XPS analysis. The base pressure in the analysis chamber was about 3×10^{-10} mbar. Typically, the hydrocarbon C1s line at 284.8 eV from adventitious carbon was used for energy referencing.

TGA was performed on Perkin-Elmer Pyris 6 at a scanning rate of 10°C/min from 40 to 800°C under nitrogen.

X-ray diffraction (XRD) patterns were recorded on a D8 ADVANCE X-ray powder diffractometer system (Bruker Corporation, German) using a tube voltage of 40 kV, a current of 40 mA, a range of 10° to 90° and a step size of 0.06°.

Fluorescence spectra were recorded on a Shimadzu RF-5301PC fluorescence spectrophotometer.

The dynamic light scattering (DLS) measurements were performed by using a commercialized spectrometer from Brookhaven BI-200SM Goniometer equipping a 17 mW He-Ne laser (633 nm). A Laplace inversion program was used to process the data to obtain the effective diameter

Synthesis of HNTs-PAM

Accurately weighed HNTs-I (20 mg) and recrystallized acrylamide (60 mg, 0.85 mmol) were added into 5 mL distilled water in a Schlenk flask. Ultrasound was used to make it well dispersed. Then the system was exposed to 365 nm LED light (Power: 35 W; Intensity: 10²mW/cm²; Distance: 10 cm) for 30 min. The residue was thoroughly washed with water and then collected by centrifugation. The product HNTs-PAM was obtained after drying in vacuum.

Synthesis of HNTs-CDs

The HNTs-PAM powders were filtered by a 200-mesh sieve. Filtered HNTs-PAM powders were physically mixed with oxalic acid in a mass ratio of 2:1 in a crucible. The mixture was heated at 100 °C for 5 min. Then the mixture was thoroughly washed with water and then dried in vacuum to afford the HNTs-CDs.

Preparation of composite films

The HNTs-PAM powders were filtered by a 200-mesh sieve. Filtered HNTs-PAM powders were physically mixed with oxalic acid in a mass ratio of 2:1 in water. Vigorous stirring was continued to afford a uniform suspension. This suspension was poured onto a glass plate and then spread uniformly via a mild shock by using a shaker rotating with the agitation rate at 100 rpm. The samples were dried at room temperature in a dark environment. The obtained films were stored in a dry box before being used.

Stability test

A WD-2A stability test instrument was used to evaluate the stability of the formed HNTs-CDs (Temperature: $60 \pm 0.5^\circ\text{C}$; Light intensity: 2000 lx, white; Humidity: $50 \pm 4\%$). The samples were placed in the stability test instrument for 7 days to evaluate the stability to heat and light stability. The photoluminescence spectra of the samples on day 0, day 1, day 3, day 5, and day 7 were recorded.

Additional data

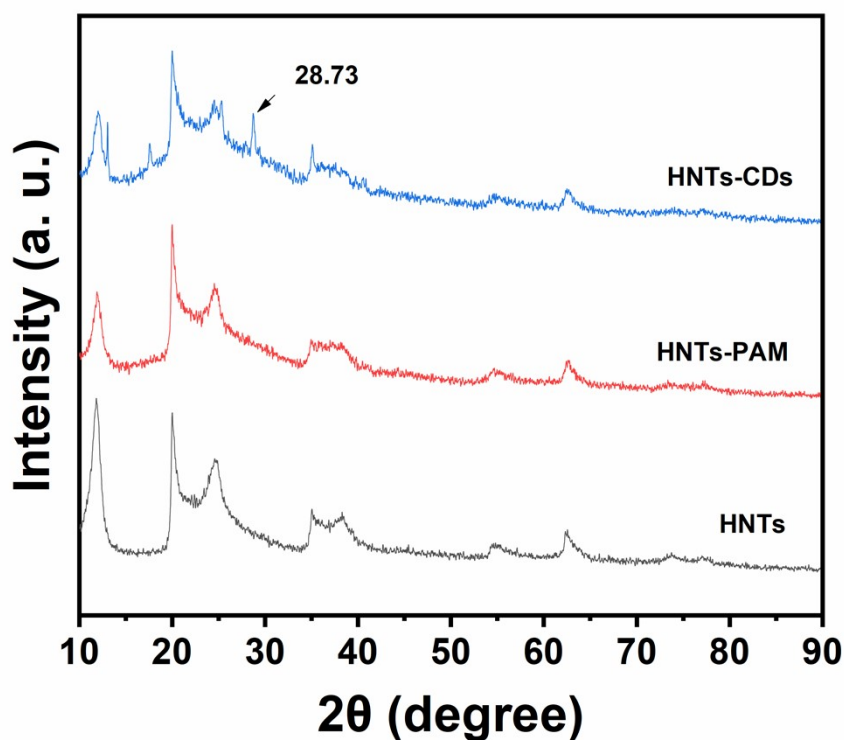


Figure S1. XRD patterns of HNTs, HNTs-PAM, and HNTs-CDs.

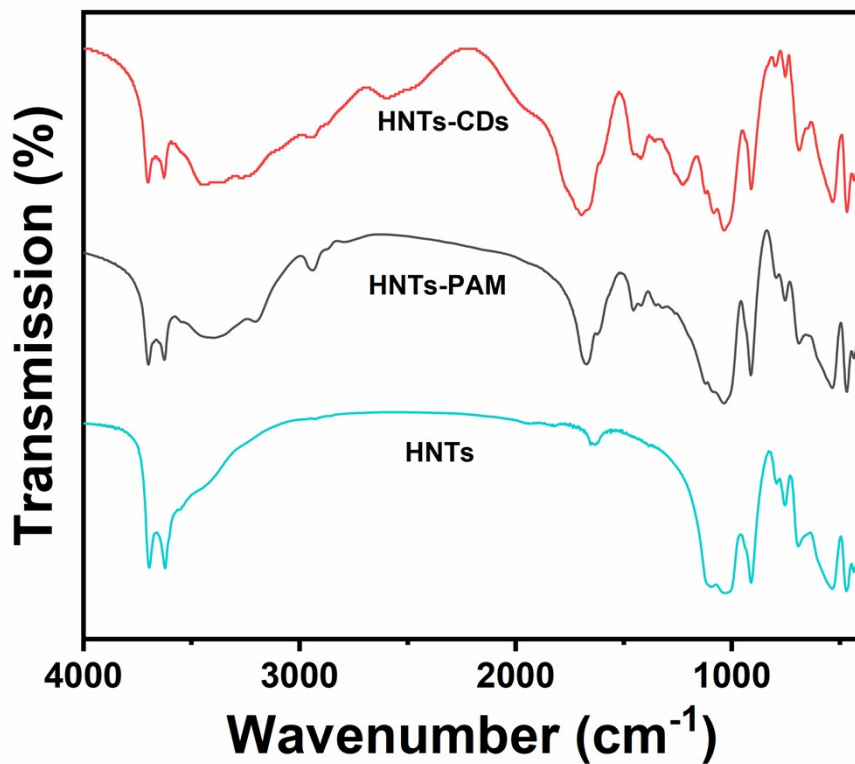


Figure S2. FTIR spectra of HNTs, HNTs-PAM, and HNTs-CDs.

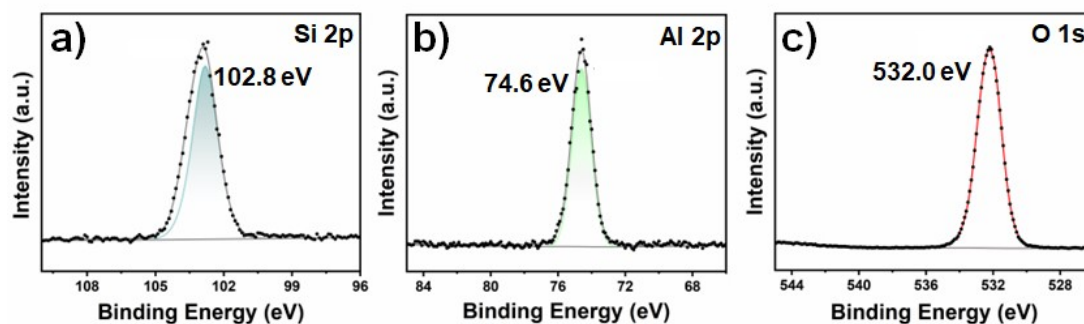


Figure S3. XPS results of HNTs used in this study. a) Si region from the XPS spectrum of HNTs. b) Al region from the XPS spectrum of HNTs. c) O region from the XPS spectrum of HNTs.

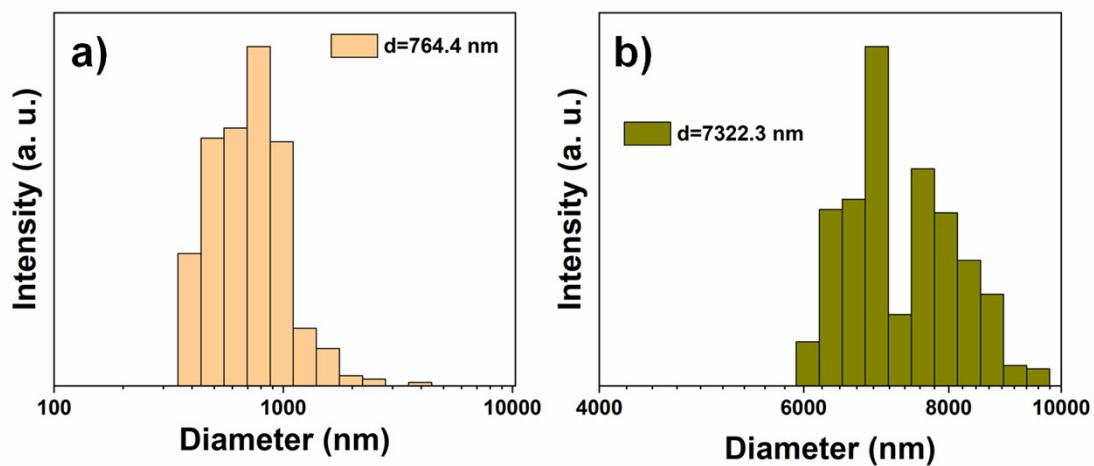


Figure S4. DLS diagrams. a) HNTs-PAM. b) HNTs-CD.

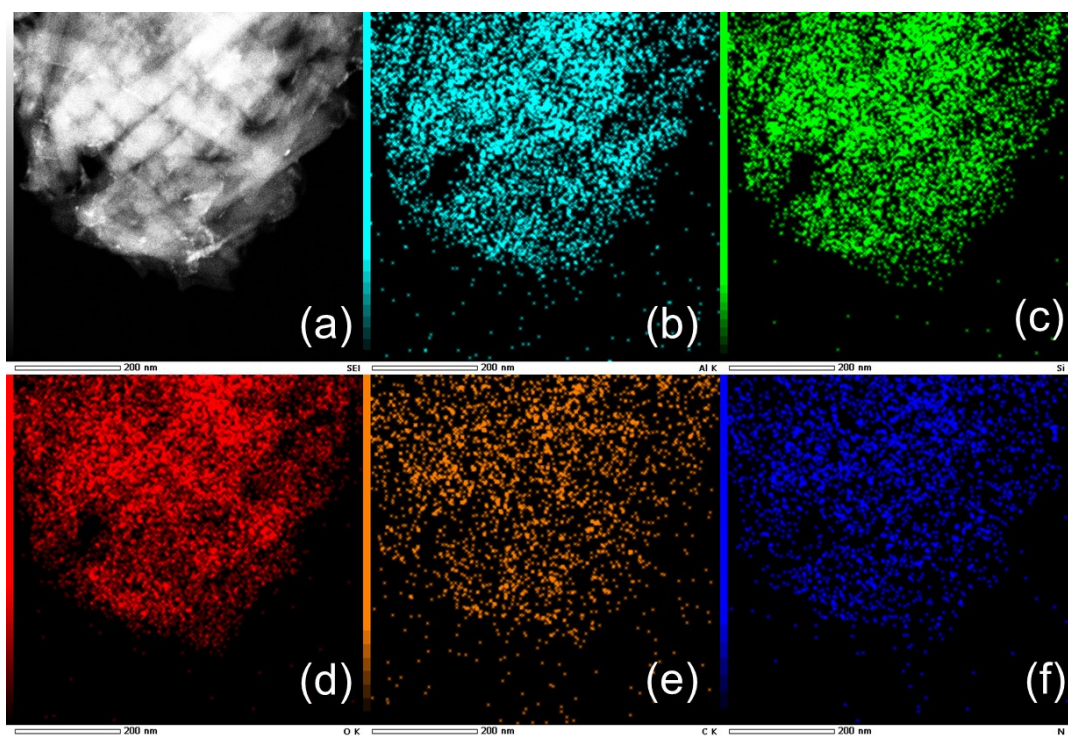


Figure S5. Elemental mapping results of the obtained HNTs-CDs. a) High-angle annular dark-field STEM image. b) Al. c) Si. d) O. e) C. f) N.

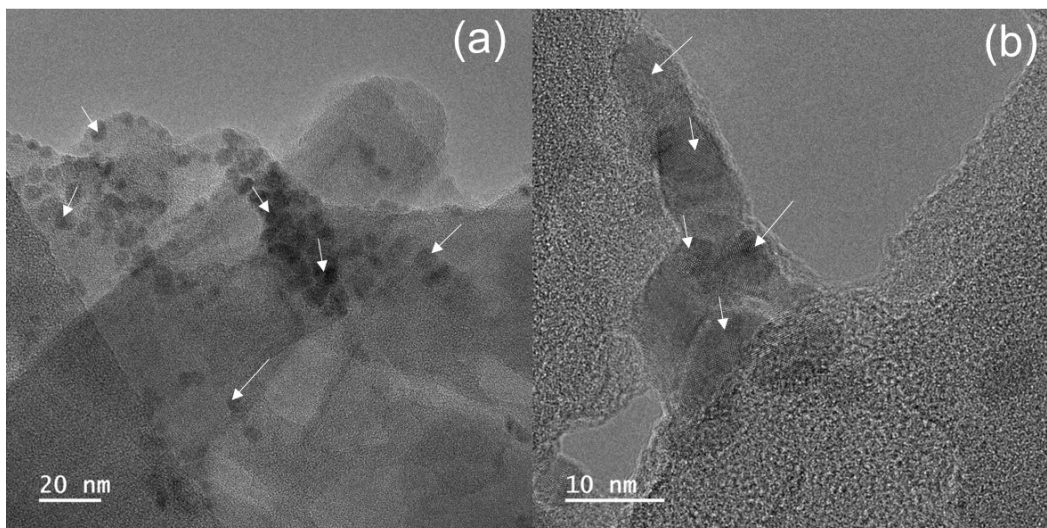


Figure S6. High-resolution transmission electron microscopy (HRTEM) images. **a)** bar = 20 nm; **b)** bar = 10 nm.

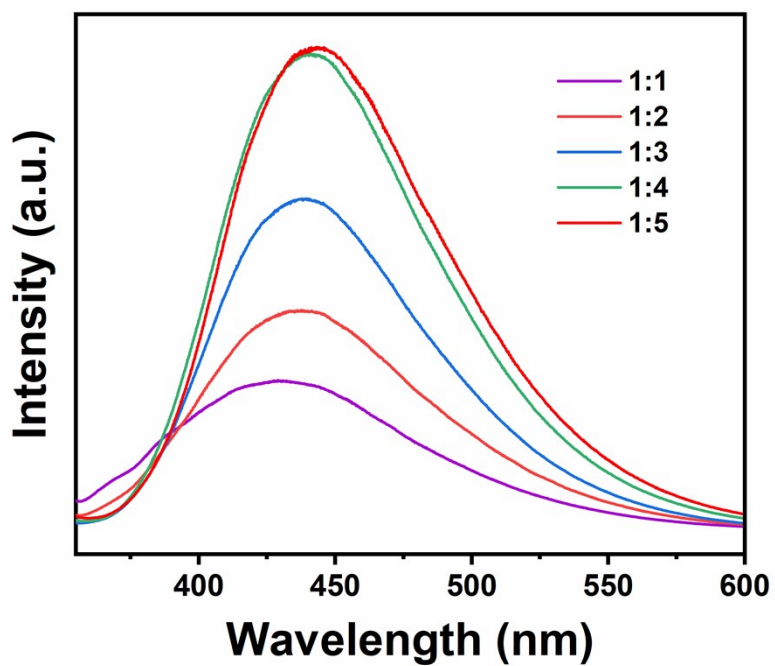


Figure S7. Photoluminescence spectra of the mixture of HNTs-PAM and oxalic acid with feed mol. ratio of $-NH_2/-COOH$ as 1:1, 1:2, 1:3, 1:4, and 1:5.

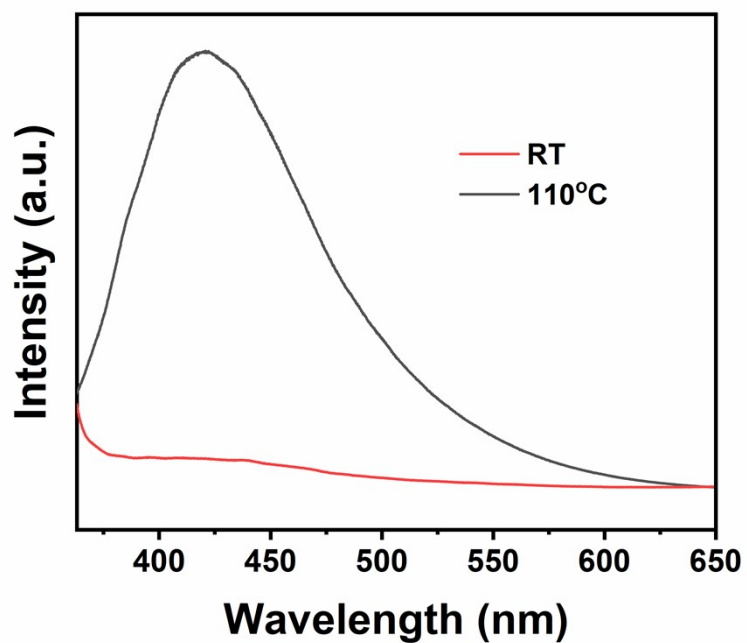


Figure S8. Photoluminescence (PL) spectra of the mixture of HNTs-PAM and malic acid at different temperatures.

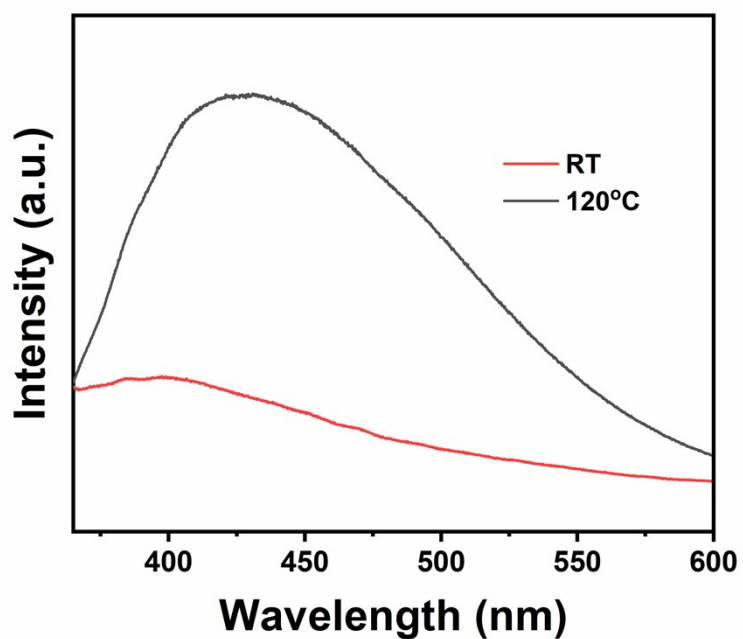


Figure S9. Photoluminescence (PL) spectra of the mixture of HNTs-PAM and tartaric acid at different temperatures.

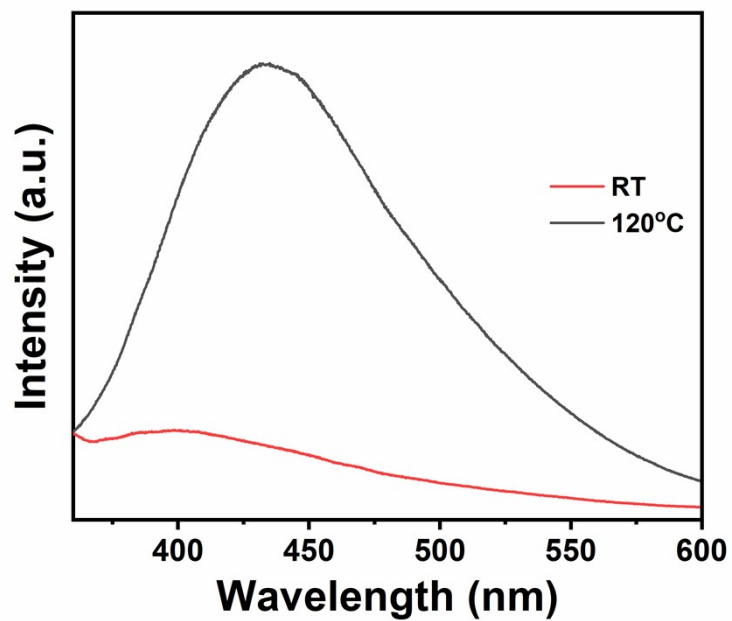


Figure S10. Photoluminescence (PL) spectra of the mixture of HNTs-PAM and citric acid at different temperatures.

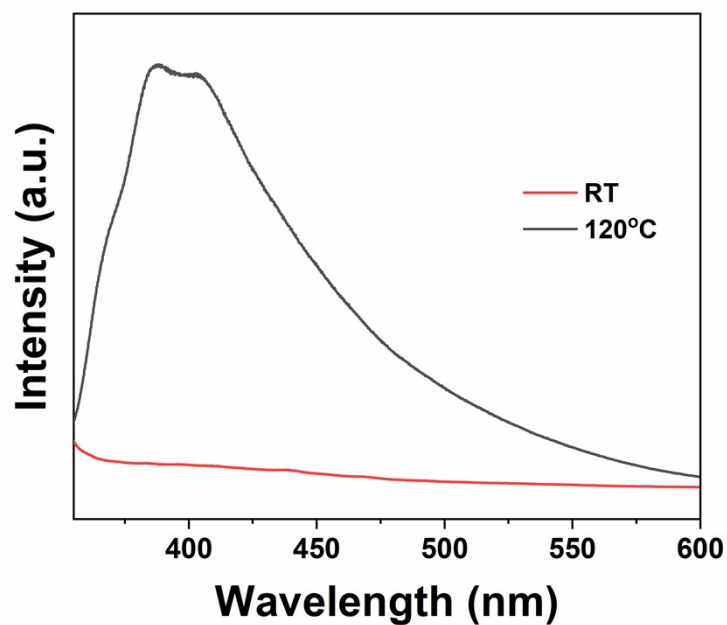


Figure S11. Photoluminescence (PL) spectra of the mixture of HNTs-PAM and butanetetracarboxylic acid at different temperatures.

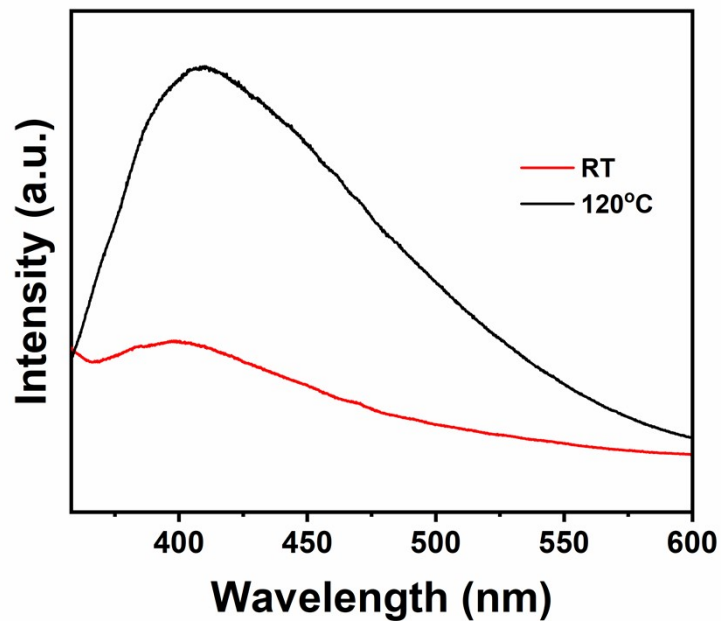


Figure S12. Photoluminescence (PL) spectra of the mixture of HNTs-PAM and L- aspartic acid at different temperatures.

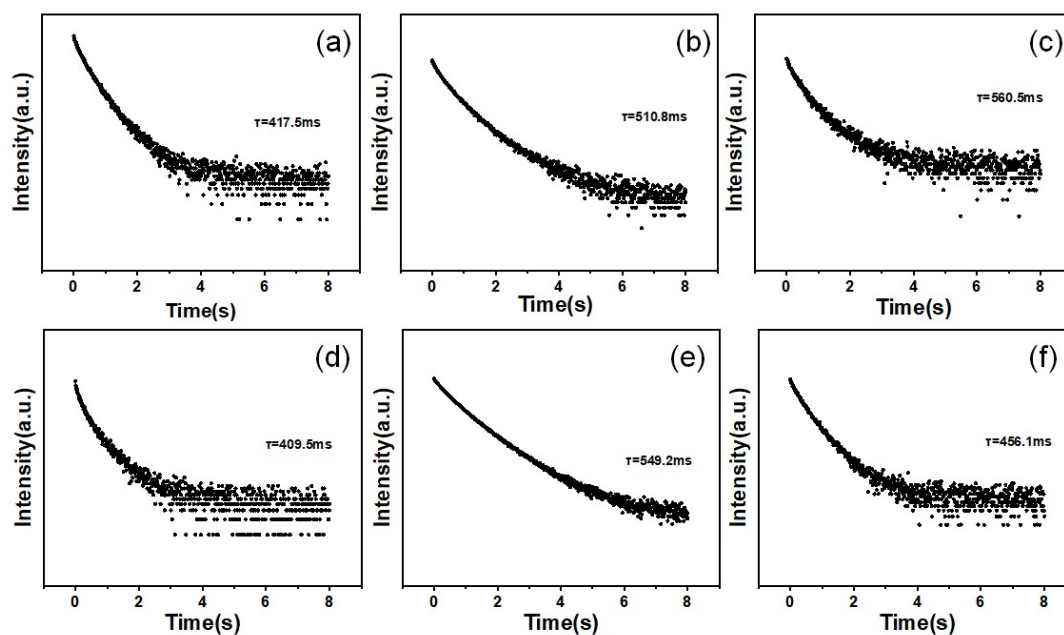


Figure S13. Phosphorescence spectra of composites prepared by treating HNTs-PAM with different kinds of polycarboxylic acids. **a)** Oxalic acid. **b)** Malic acid. **c)** Tartaric acid. **d)** Citric acid. **e)** Butanetetracarboxylic acid. **f)** L- aspartic acid.

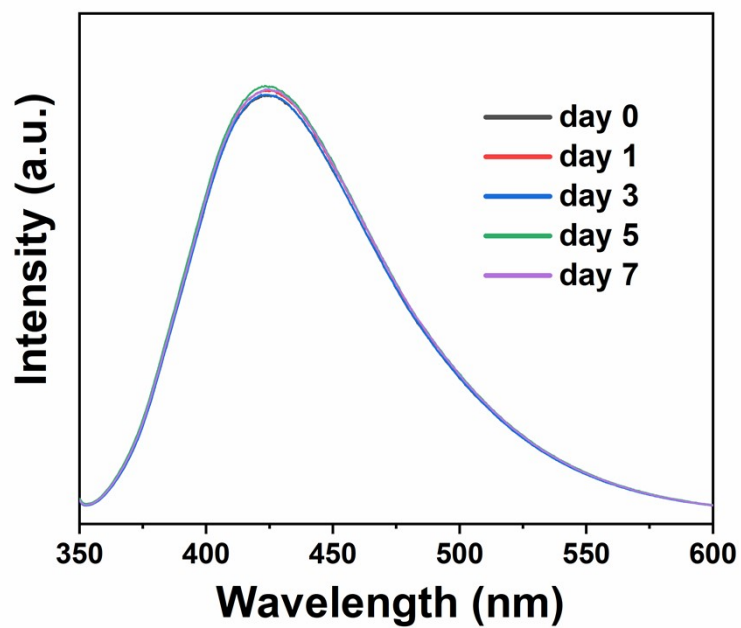


Figure. S14. Photoluminescence spectra of the HNTs-CDs in stability test.

Reference

1. Y. Wang, X. Ba, B. Zhang, Y. Wang, Y. Wu and H. Zhang, *J. Colloid Interface Sci.*, 2024, **657**, 344-351.
2. Y. Lu, H. Zhao, X. Huang, D. Hu, Y. Wu, X. Ba and H. Zhang, *Chem. Commun.*, 2022, **58**, 13636-13639.